

Supplementary information

Theoretical densities of the single phase materials

Theoretical densities of the single phase materials ρ_{theo} are calculated to

$$\delta_{theo} = [Z M] / [A V] \quad (S1)$$

(A – Avogadro’s constant, M – molar mass, V – unit cell volume, Z – formula units per unit cell). For the compositions $x = \{2, 2.72, 2.90, 3\}$ the unit cell volume V is gained from the lattice parameter refinements in this work, otherwise from literature data (Table 1, main text).

For $x = 2.90$ we find a discrepancy: The density $\rho_{theo} = 7.16 \text{ g cm}^{-3}$ is based on *Magnéli’s* model with perfectly undistorted $[\text{WO}_6]$ octahedra between the CS planes [35]. This represents the least dense packing of the octahedra. Thus, every real structure wherein tilting and distortion occur must yield a density $\rho_{theo} > 7.16 \text{ g cm}^{-3}$ as observed in previous experimental work [11, 21]. However, we gain a ρ_{theo} from the PXRd data which is considerably lower than predicted by *Magnéli’s* model. Also none of the published values clearly exceeds the density of the room temperature phases γ - WO_3 (7.19 g cm^{-3}) and δ - WO_3 (7.29 g cm^{-3}) although the CS planes in $\text{WO}_{2.90}$ are supposed to result in a distinct compression of the WO_3 parent structure [42].

Table S1. Mass density ρ_{theo} of tungsten oxides calculated from their molar mass M and unit cell volume V (see **Table 1** in main text). The relative mass density ρ_{rel} is obtained by measuring the density ρ_m .

X	M g mol ⁻¹	Phase	Z	ρ_{theo} g cm ⁻³	ρ_m g cm ⁻³	ρ_{rel} %	Ref.
2	215.84	WO ₂	4	10.77	-	-	[30]
			4	10.78	9.64	89.42	this work
2.72	4093.12	W ₁₈ O ₄₉	1	7.69	n.a.	n.a.	[31]
			1	7.71	n.a.	n.a.	[32]
			1	7.73	n.a.	n.a.	[33]
			1	-	7.70	100	[11]
			1	7.72	7.49	97.02	this work
2.90	4604.80	W ₂₀ O ₅₈	1	7.17	-	-	[21]
			1	7.16	-	-	[35]
			1	7.20	6.95	98	[11]
			1	7.11	7.05	99.12	this work
2.92	5580.16	W ₂₅ O ₇₃	2	6.88	-	-	[14]
3	231.84	ϵ -WO ₃	4	7.39	-	-	[43]
		δ -WO ₃	8	7.29	-	-	[44]
		δ - & γ -WO ₃	-	-	7.19	-	this work
		γ -WO ₃	8	-	-	-	this work
		γ -WO ₃	8	7.19	-	-	[36]
		β -WO ₃	8	7.12	-	-	[36]
α -WO ₃	8	7.03	-	-	[36]		

Thermoelectric properties

In **Figure S1a** the electrical conductivities of the known compositions $x = 2, 2.72$ and 2.90 are compared. $\text{WO}_{2.90}$ shows $\sigma(T) = 77(4) \cdot 10^3 \text{ S m}^{-1}$ over the whole temperature range and a local maximum at 635 K. WO_2 and $\text{WO}_{2.72}$ reveal a metallic behaviour with the typical dependency $\sigma(T) \propto 1/T$ over a wide temperature range (**Figure S1b**).

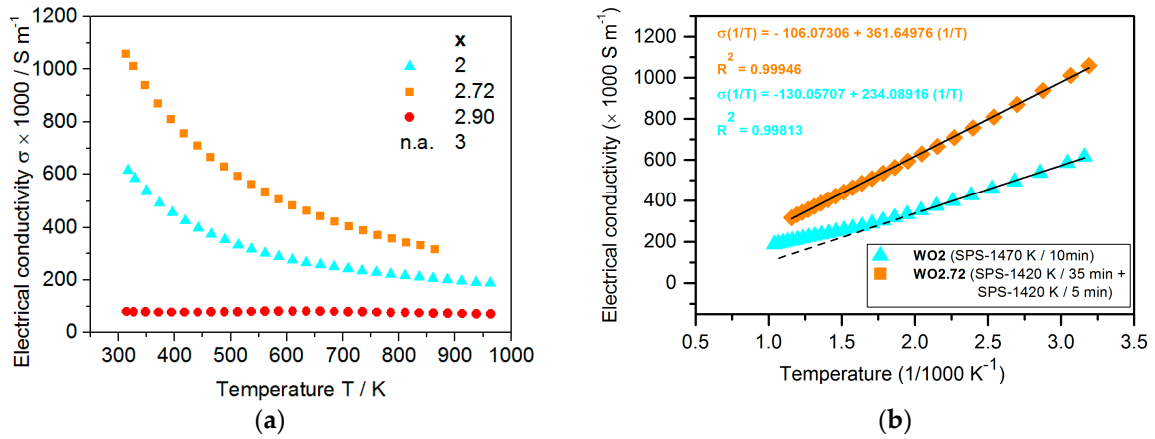


Figure S1. (a) Electrical conductivity $\sigma(T)$ of the reference materials WO_2 , $\text{WO}_{2.72}$ and $\text{WO}_{2.90}$. No measurement was possible for WO_3 due to its insulating character. (b) A linear interpolation (black line) shows the metallic behaviour of WO_2 and $\text{WO}_{2.72}$ with $\sigma(T) \propto 1/T$ dependency. An extrapolation (dashed lines) reveals a deviation from this behaviour for WO_2 at high temperatures $T > 500 \text{ K}$.

As expected due to its semiconducting behaviour $\text{WO}_{2.90}$ exhibits the highest negative Seebeck coefficient among the known compositions (Figure S2a). Therefore $\text{WO}_{2.90}$ also shows the highest figure of merit ZT for temperatures $> 535 \text{ K}$ whilst for $T < 535 \text{ K}$ the low electrical conductivity is disadvantageous and $\text{WO}_{2.72}$ exhibits the higher ZT (Figure S2b).

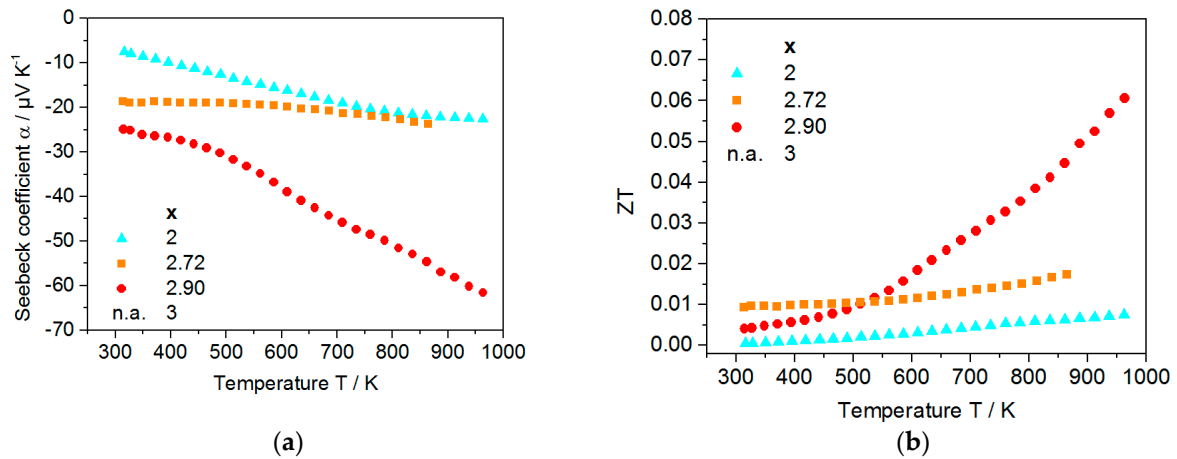


Figure S2. (a) Seebeck coefficient $\alpha(T)$ and (b) the resulting figures of merit ZT of the reference materials WO_2 , $\text{WO}_{2.72}$ and $\text{WO}_{2.90}$. No measurement was possible for WO_3 due to its insulating character.

Reference sample $\text{WO}_{2.90}$

In the samples WO_x prepared with SPS-1420 K / 10 min we find the phase “ $\text{WO}_{2.82}$ ” for $2.72 \leq x \leq 2.90$ which might be $\text{W}_{12}\text{O}_{34}$. This phase cannot be formed due to SPS-specific effects since it is also observed in $\text{WO}_{2.90}$ material which was synthesized in an evacuated silica tube for 72 h at 1370 K (Figure S3a).

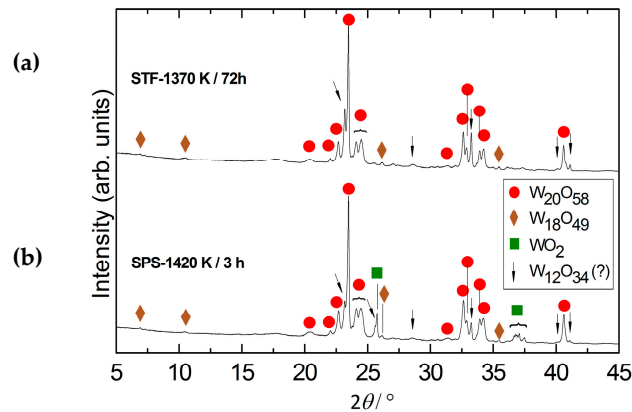


Figure S3. PXRD patterns of $\text{WO}_{2.90}$ obtained (a) from heating in an evacuated silica tube at 1370 K for 72 h and (b) from SPS synthesis at similar temperature for 3 h. Reflections of the new phase “ $\text{WO}_{2.82}$ ” which might be $\text{W}_{12}\text{O}_{34}$ appear for both routines. Radiation was $\text{Cu-K}\alpha_1$.

c_p measurements of WO_x materials from differential scanning calorimetry (DSC)

Preliminary $c_p(T)$ measurements were performed for WO_x materials which were synthesized with SPS-1320 K / 10 min. Differences between the measured $c_p(T)$ values were non-systematic and smaller than the 10 % error of the *DSC 404 C Pegasus* (Netzsch, Selb, Germany) device (Figure S4, error bars). Thus, for calculations of the thermoelectric properties of WO_x and WO_2 theoretical values of WO_3 and WO_2 from the *NIST-JANAF* database were used respectively (Figure S4, dotted lines).

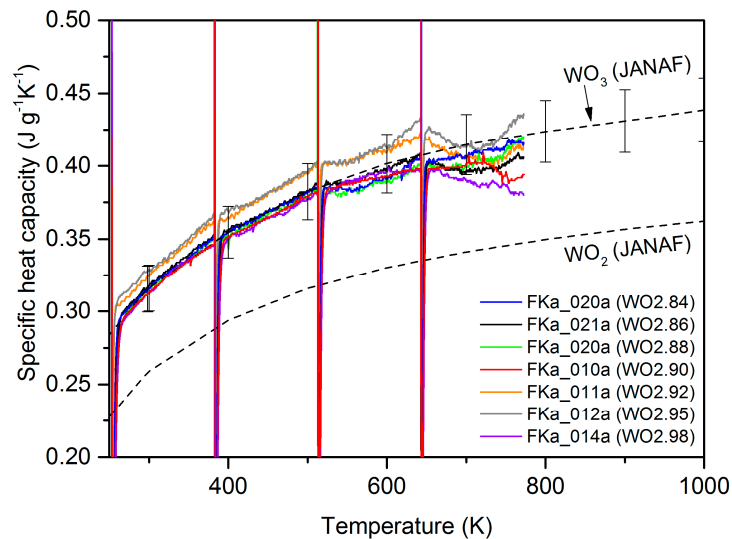


Figure S4. Specific heat capacity $c_p(T)$ of WO_x materials show values close to calculations from the *NIST-JANAF* database (dotted lines) and differed by less than 10 % (error bars).